

Application of systematic monitoring and mapping techniques: Assessing land restoration potential in semi-arid lands of Kenya



Leigh Ann Winowiecki^{a,*}, Tor-Gunnar Vågen^a, Margaret F. Kinnaird^b, Timothy G. O'Brien^c

^a World Agroforestry Centre (ICRAF), Nairobi, Kenya

^b World Wildlife Fund for Nature (WWF), Nairobi, Kenya

^c Wildlife Conservation Society (WCS), Bronx, USA

ARTICLE INFO

Handling Editor: A.B. McBratney

1. Introduction

Drylands cover over 40% of the earth's surface and support over 2 billion people, globally (Millennium Ecosystem Assessment, 2005). In East Africa alone, over 250 million people depend on drylands for their livelihoods (De Leeuw et al., 2014) and in Kenya, 70% of the total land area is classified as arid- and semi-arid (Batjes, 2004). Over the last several decades, an increasing and more sedentary human population has resulted in more pressure on these lands, and an expansion of agricultural production into marginal dryland areas that were traditionally rangelands. The result is widespread soil loss and land degradation, as well as increased pressure on protected areas and more frequent human-wildlife conflict in Kenya (Laikipia Wildlife Forum, 2012; Nyamwamu, 2016). These factors, combined with climate change and erratic rainfall, continue to increase the vulnerability of drylands in East Africa (Darkoh, 1998). However, drylands are also considered to have an important role in mitigating climate change (Lal, 2004; Neely et al., 2009; Neely and De Leeuw, 2008), are important biodiversity hot-spots and support a diversity of livelihoods (Mortimore, 2009). While land degradation is recognized as a major cause of low agricultural and rangeland productivity, estimates of land degradation within the drylands remain poor and hence also vary widely. For example, the (Millennium Ecosystem Assessment, 2005) estimated that between 10% and 70% of global drylands are degraded. The application of remote sensing, coupled with systematic field assessments, for monitoring, assessing and mapping land degradation patterns and severity within landscapes has the potential to significantly improve current estimates of land degradation, while at the same time allowing for spatially explicit targeting of restoration options and monitoring of change over time. Such advances will also ultimately make assessments of the drivers of land degradation in drylands possible, which is critical for successful restoration and for avoiding further degradation.

Several studies highlight soil erosion as an important process of land degradation (Dregne, 2002; Mortimore, 2009; Tiffen and Mortimore, 2002; Vågen et al., 2013a), and as important indicator of land health due to its negative impacts on soil health and overall land productivity. Furthermore, poor agricultural and rangeland management practices are leading to loss of soil organic carbon (SOC), mining of soil fertility, increased soil compaction, as well as water and wind erosion. These processes, which are often confounded by climate change and the high levels of susceptibility to degradation in drylands often result in loss of overall system productivity and resilience even under moderate stress (Darkoh, 1998; Vågen et al., 2013b; Vågen and Gumbritch, 2012). Degraded lands, continually put into production, without restoration or other conservation measures, can become irreversibly unproductive, jeopardizing the livelihoods of millions of people who depend on these systems. Thus, ecosystem restoration has become an important field of research (Aronson and Alexander, 2013; Crouzeilles et al., 2016; Dobson et al., 1997; Itto, 2002; IUCN and WRI, 2014; Lapstun, 2015; Suding et al., 2015; Williams-linera et al., 2011; Young et al., 2005), especially in dryland areas (FAO, 2015; Herrick et al., 2013; Riginos and Herrick, 2010).

A growing number of international initiatives are dedicated to restoration of degraded lands, most notably the Bonn Challenge (www.bonnchallenge.org) and AFR100 (www.afr100.org). In addition, the concept of land degradation neutrality (LDN) was adopted as a target for Sustainable Development Goal (SDG) 15 (Cowie et al., 2018; UNCCD, 2016). Sustainable Development Goal (SDG) 15 aims to “protect, restore and promote sustainable use of terrestrial ecosystems, sustainably manage forests, combat desertification, and halt and reverse land degradation and halt biodiversity loss”. Indicators agreed upon included trends in land use/cover, land productivity and soil organic carbon stocks. In order to support this agenda, methods and approaches that are scientifically rigorous and applicable to a range of

* Corresponding author.

E-mail address: l.a.winowiecki@cgiar.org (L.A. Winowiecki).

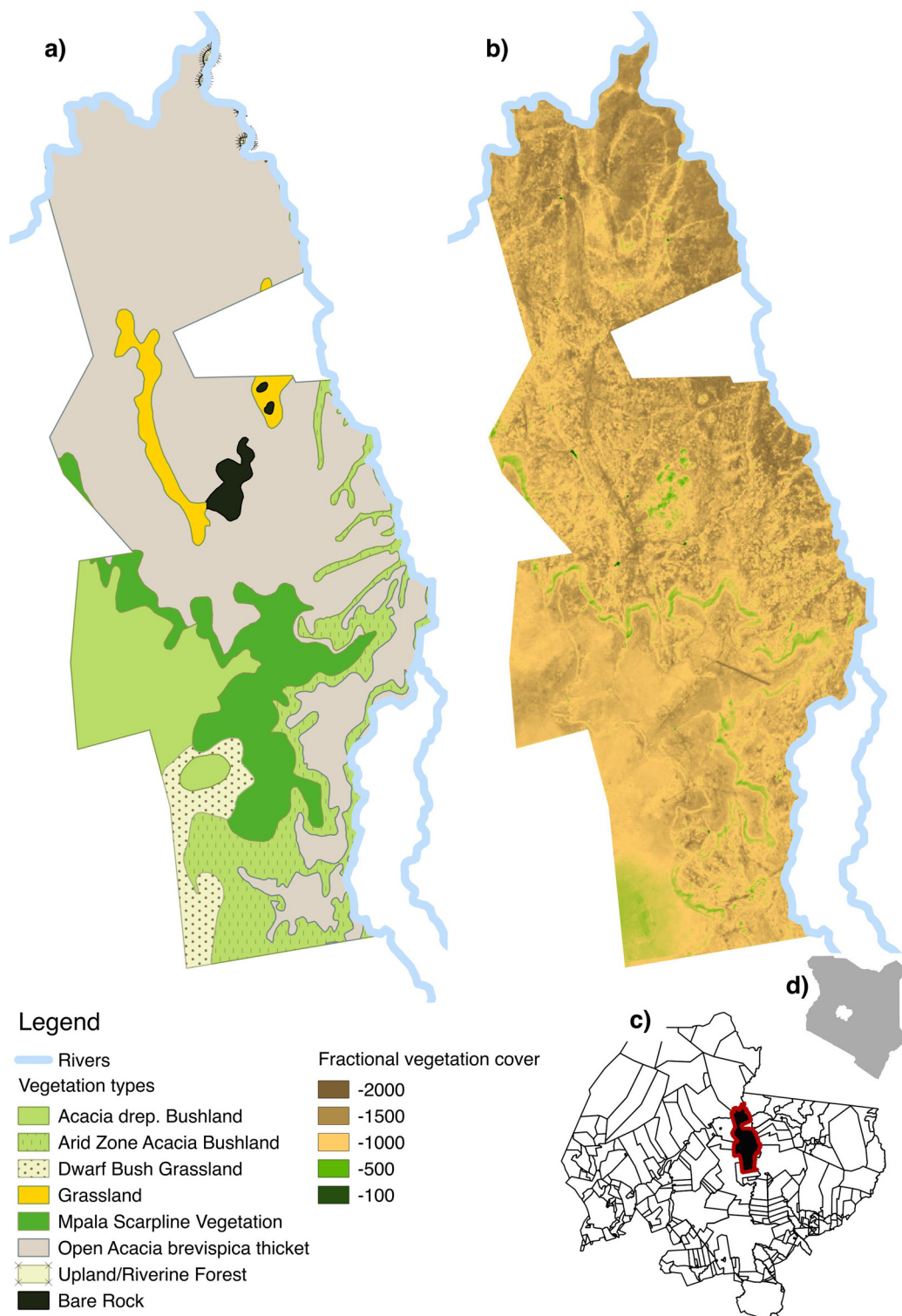


Fig. 1. Overview maps showing: a) Vegetation classes in Mpala Ranch b) Fractional vegetation cover across Mpala ranch, calculated using Soil Adjusted Total Vegetation Index (SATVI); c) Map of the administrative boundaries within Laikipia county with the location of Mpala Ranch highlighted; and d) Map of Kenya, showing the location of Laikipia county in white.

different ecosystems at multiple scales are needed to assess and monitor land degradation. To aid country practitioners in carrying out restoration activities, the International Union for the Conservation of Nature (IUCN) and the World Resources Institute (WRI) created a guide to assess opportunities for forest landscape restoration, where they highlight the need for more reliable spatial data for assessing restoration potential (IUCN and WRI, 2014). However, major gaps still exist in

methods to assess land degradation, particularly for spatially explicit assessments at scales necessary for targeting interventions (Davies et al., 2012; Lal, 2004; Mortimore, 2009).

In the current paper we apply a systematic approach to the assessment of land health with a case study in a Kenyan dryland system in Laikipia County. We argue that such a systematic approach is critically important for addressing the challenges of land degradation, for

targeting of restoration efforts, and for monitoring of trends over time, across multiple spatial scales. Laikipia County is an excellent example of a dryland region characterized by a mosaic of land management approaches ranging from wildlife conservancies to commercial livestock ranches, pastoral lands and croplands. Continued grazing pressure and increasing conflicts with wildlife add to the complexity of managing these lands (Kinnaird and O'Brien, 2012). The Laikipia Wildlife Forum (LWF), a members' network comprised of local stakeholders, and a number of outside organizations have had mixed success in assisting Laikipia landowners/users with erosion control and grassland regeneration (Riginos et al., 2012). Most of these interventions have been small scale and few include long-term monitoring of progress, underscoring the need for targeted restoration. The Strategic Target 3.2 of The Wildlife Conservation Strategy for Laikipia County further stresses the need to “maintain or enhance areas of natural habitat that are currently vulnerable or in decline” through better range management with systematic and coordinated monitoring (Laikipia Wildlife Forum, 2012).

While several initiatives agree that systematic biophysical assessments across rangeland sites are needed (Karl and Herrick, 2010; Riginos and Herrick, 2010; Schwilch et al., 2014, 2011), few have conducted spatially explicit assessments using scientifically rigorous indicators and analytical frameworks. For example, digital soil mapping techniques can be applied to assess interactions between soil properties and processes of land degradation, which is critical for identifying degraded areas, assessing the severity of degradation and for designing restoration interventions that are spatially explicit and effective. In other words, landscape-scale assessments and mapping of biophysical indicators of land degradation and soil health are critically needed to better understand relationships between factors such as aboveground vegetation structure and diversity, soil health and soil erosion. Furthermore, identifying thresholds or tipping points for indicators such as vegetation cover, soil organic carbon (SOC) and soil erosion is important to design management strategies to improve soil health and increase land productivity across semi-arid landscapes.

We chose Mpala Ranch, a commercial livestock ranch and wildlife conservancy in Laikipia County in Kenya as a case study to apply digital soil mapping techniques to identify and target restoration “go to” areas. We applied a combination of systematic field surveys, including soil data collection, and remote sensing to address four principal objectives in this study: 1) Conduct a baseline assessment of soil and land health indicators for Mpala Ranch; 2) Assess the variation in SOC under different vegetation classes; 3) Create predictive surfaces (maps) of SOC and erosion; and 4) Assess restoration potential across the Mpala landscape.

2. Methods

2.1. Site description

We conducted our assessment on the 200 km² Mpala Ranch, located in the western sector of Laikipia County, Kenya (0°22'44" N, 36°53'43" E) (Fig. 1). Laikipia County is approximately 10,000 km² and is part of the ~56,000 km² Greater Ewaso Ecosystem (Georgiadis et al., 2007). Rainfall varies from 900 mm yr⁻¹ at the equator to < 400 mm yr⁻¹ in the north; most of the population and agricultural activities are located in the south where rainfall exceeds 500 mm yr⁻¹. In the north, livestock production and wildlife management predominate. Land holdings are almost entirely private properties and include group or community held ranches, private cattle ranches and conservancies, traditional grazing lands for pastoralists and rhinoceros sanctuaries. Cattle stocking densities range from 0 to > 25 total livestock units km⁻² (Kinnaird and O'Brien, 2012), and can increase even higher during the dry season and droughts when pastoralists from outside Laikipia move in. The diversity of land use provides a gradient against which to assess the impact of land management on SOC and land degradation risk. Mpala Ranch is an

active cattle ranch that also manages for wildlife, and hosts an international research center. Mpala Ranch contains five major vegetation classes: *Acacia drepanolobium* bushland (ADB), arid zone mixed *Acacia* bushland (AZMAB), open *Acacia brevispica* thicket (ABT), grasslands (GR) and Mpala scarpline vegetation (MSV) (Young et al., 1997, Center for Training and Integrated Research in ASAL Development and Mpala Research Centre Unpublished Data) (Fig. 1). Soils are broadly classified as black cotton soil, related to the *Acacia drepanolobium* bushland (Ahn and Geiger, 1987; Young et al., 1998), red soils associated with all habitat classes except *Acacia drepanolobium* bushland, and transition soils associated with all habitat classes except arid zone mixed *Acacia* bushland (Ahn and Geiger, 1987).

2.2. Biophysical field sampling

The Land Degradation Surveillance Framework (LDSF) (T-G. Vågen et al., 2013) was used to sample a 100 km² site within Mpala Ranch. The LDSF is designed for practical and cost-effective soil and ecosystem health surveillance, and for mapping SOC and soil erosion prevalence, in particular (Tor-G Vågen et al., 2013; Vågen et al., 2012; Vågen and Winowiecki, 2013; Winowiecki et al., 2016). The framework is also designed for monitoring changes over time, and provides opportunities for targeting improved soil management and land restoration activities. Specifically, the LDSF is unique in that it systematically assesses several ecological metrics simultaneously at four different spatial scales (100 m², 1000 m², 1 km², 100 km²), using a spatially stratified, hierarchical sampling design (Vågen et al., 2013b).

For example, field observations were made at both plot-level (1000 m² circular plots) and subplot-level (100 m² circular plots). At each plot ($n = 160$ per site) observations of slope (in degrees), vegetation structure using the FAO Land Cover Classification System (forest, woodland, bushland, shrubland, wooded grassland, grassland, or cropland) (Di Gregorio and Jansen, 1998), topographic position (upland, ridge/crest, midslope, footslope or valley), land management and land-use history were made. Visible observations and classification of soil erosion prevalence were made within each circular subplot ($n = 4$ per plot, 640 per site), (e.g., gully erosion, rill erosion, sheet erosion or none). These soil erosion observations were used to compute a plot-level severe erosion index (e.g., if 3 or 4 subplots per plot had visible signs of erosion than the severe erosion score for the plot was “1”, otherwise, the “0”). Trees in the LDSF were classified as woody vegetation over three meters tall, while shrubs were classified as woody vegetation between 1.5 and 3 m in height. All trees and shrubs within each subplot were counted ($n = 640$ per site) and used to calculate tree and shrub densities. In addition, herbaceous and woody cover ratings were made using the Braun-Blanquet scale from 0 (bare) to 5 (> 65%) (Braun-Blanquet, 1932). Composite soil samples were collected at each plot using soil augers, combining topsoil (0–20 cm) samples from each of the four subplots into one sample and the four subsoil (20–50 cm) samples into one subsoil sample per plot. A total of 160 topsoil samples and 160 subsoil samples were collected from a full LDSF site (total = 320 samples). All soil samples were transported to the World Agroforestry Centre (ICRAF) Soil-Plant Spectral Diagnostics Laboratory in Nairobi, Kenya directly after sampling.

2.3. Soil laboratory analysis and mid-infrared spectroscopy (MIRS)

Soil samples were air-dried then ground to pass through a 2-mm sieve. Soil samples analyzed for mid-infrared (MIR) absorbance were further processed by (i) taking a subsample of ~10 g for further drying at 40 °C for 24 h, (ii) grinding the dried samples using a RM 200 Retsch motor grinder to attain a particle size between 20 and 53 µm, and (iii) loading three subsets of the sample (about 1–2 g each) onto an aluminum sample plate. MIR absorbance was measured on a Tensor 27 HTS-XT instrument from Bruker Optics at the ICRAF Soil-Plant Spectral Diagnostics Laboratory in Nairobi, Kenya. Measured wavebands ranged

from 4000 to 601 cm^{-1} with a resolution of 4 cm^{-1} . MIR is a widely used methodology for predicting important soil properties such as SOC, pH, base cations and texture (Brown, 2007; Madari et al., 2006; Reeves III et al., 2006; Shepherd and Walsh, 2002; Terhoeven-urselmans et al., 2010; Vågen et al., 2006). The ICRAF GeoScience Laboratory has a MIR spectral database with over 80,000 soil spectra. Soil samples that had both MIR spectra and wet chemistry data were used to develop MIR prediction models for the various soil properties (Vågen et al., 2016), and is further elaborated in Section 2.4. Processing of the MIR spectra followed the procedures outlined in Terhoeven-urselmans et al. (2010), with first derivatives computed using a Savitsky-Golay polynomial smoothing filter implemented in the *locpoly* function of the *KernSmooth* R package (Wand, 2015) prior to prediction model development.

The use of MIRS allows for rapid and low cost soil analysis as only 10% of the soil samples from an LDSF site are analyzed using traditional wet chemistry methods (see Section 2.4). A random subset of 32 standard top- and subsoil samples were analyzed for OC, pH, exchangeable bases and texture using traditional wet chemistry methods (e.g., topsoil and subsoil samples from one reference plot per cluster ($n = 16$ clusters) for a total of 32 soil samples from the LDSF site). pH was analyzed in a 1:2 H_2O mixture (20 g of soil: 40 mL de-ionized water) that was shaken for 30 min at moderate speed on a horizontal shaker then let stand for 20 min before reading on a Eutech Cyberscan 1100 pH meter. Exchangeable bases were extracted using a Mehlich-3 method (Mehlich, 1984) (4 g of soil in 40 mL of the Mehlich 3 extracting solution) after being shaken for 5 min on a reciprocating shaker. The filtrate was analyzed for base cations: potassium (K), calcium (Ca), magnesium (Mg) and sodium (Na) on ICP OES (Model-Thermo *iCAP6000 Series*) at Crop Nutrition Laboratory Services in Nairobi, Kenya. Total N and OC were measured by dry combustion using an Elemental Analyzer Isotope Ratio Mass Spectrometry (EA-IRMS) instrument from Europa Scientific after removing inorganic C with 0.1 N HCl, at the IsoAnalytical Laboratory located in the United Kingdom. Clay content was measured using a Laser Diffraction Particle Size Analyzer (LDPSA) from HORIBA (LA 950) after shaking each soil sample for 4 min in a 1% sodium hexametaphosphate (calgon) solution, at the World Agroforestry Centre (ICRAF) Soil-Plant Spectral Diagnostics Laboratory in Nairobi, Kenya.

2.4. Statistical analysis

2.4.1. Prediction of soil properties from MIRS

Soil properties were predicted using a random forest (RF) (Breiman, 2001) model for each of the soil properties included in the study based on the first derivative of the MIR spectra described earlier. The use of RF models for predicting soil properties is also described in Vågen et al. (2013). In brief, RF modeling is an ensemble modeling approach, where in the case of this study many decision trees are combined or bagged to predict the different soil properties based on MIR absorbance. The ICRAF MIR database, which consisted of about 3939 soil MIR spectra with matching reference soil samples (e.g., 16 topsoil and 16 subsoil samples from each LDSF site) from 123 LDSF sites was used to develop the soil property prediction models. The calibration models developed using these MIR spectra and reference samples were then applied to the MIR spectra from Mpala and validated against the 32 reference samples collected at the Mpala LDSF site.

2.4.2. Assessing the effects of vegetation types on SOC

The effects of vegetation cover types on SOC were assessed using a linear mixed effects (*lme*) model with $\ln(\text{SOC})$ as the dependent variable, vegetation classes, woody cover and herbaceous cover as the independent variables. Sampling clusters were included as random effects in the model. We chose a mixed-effects modeling approach because of the hierarchical nature of the data, and the need for an approach that takes the grouping effects in the data into account.

2.4.3. Prediction of soil properties using Landsat reflectance data

Landsat 8 (LC8) imagery from January 2015 were downloaded from the United States Geological Survey (USGS) and Operational Land Imager (OLI) bands were calibrated to top-of-atmosphere (TOA) planetary reflectance using the following equation, correcting for the sun angle:

$$\rho\lambda' = \frac{M\rho \cdot Q_{cal} + A\rho}{\sin(\theta_{se})}$$

where $\rho\lambda'$ is TOA spectral reflectance, $M\rho$ is a band-specific multiplicative rescaling factor, and $A\rho$ is a band-specific additive rescaling factor. Q_{cal} is the product digital number (DN) and θ_{se} is the local sun elevation angle. Imagery from the month of January was used because this corresponds to the dry season in the region, which has low cloud contamination, better image quality and corresponds to dry season field data collection.

Prediction models for SOC and soil erosion were then developed by extracting TOA calibrated band reflectance values for each LC8 image band and building a spectral library of LC8 band values for the field surveyed plots in the LDSF database, dropping plots where the LC8 band quality assessment band shows cloud cover. Random forest models were developed for SOC and soil erosion, using a library of LC8 reflectance values from a total of 77 LDSF sites with LC8 reflectance values (11,683 survey plots), using 70% of the data for model calibration and the remaining 30% for validation of the prediction model. The calibration and validation datasets were randomly drawn, without replacement.

Model performance for the prediction of soil erosion prevalence was assessed by calculating the receiver operator characteristic (ROC) curve for predicted versus measured soil erosion. This approach graphs sensitivity on the y-axis and 1-specificity on the x-axis, which represent the fractions of true positives and false positives in the validation predictions of soil erosion, respectively. A perfect test would have sensitivity = 1 and 1-specificity = 0. We also calculated the area under the ROC curve (AUC), which is 1 for a perfect test and 0.5 in cases where the prediction model is performing very poorly. An AUC value that is higher than 0.8 indicates good model performance, while values higher than 0.9 would indicate excellent performance.

Prediction model performance for SOC was assessed by both calculating the r^2 for predicted versus measured values for both the calibration and validation datasets, as well as root-mean-squared errors of prediction (RMSEP). Difference measures such as RMSEP summarize the mean difference of the units of measured and predicted values and generally give a reasonable picture of how the model is performing. By running these calculations on both the calibration and the validation datasets, we also get a measure of the stability of the calibration model, which is critical for predictive modeling.

Finally, the prediction models were applied to a LC8 scene from January 2015, producing maps of estimated soil erosion prevalence and SOC, respectively for the Mpala ranch.

All calculations and statistical analysis were conducted using R statistics (R Core Team, 2015) and KNIME (Berthold et al., 2007), while map layouts were made in QGIS.

3. Results and discussion

3.1. Tree and shrub densities

A total of 157 plots were sampled in the Mpala ranch, three plots were not sampled in cluster 16, due to logistical circumstances. All LDSF data are available on the World Agroforestry Centre- ICRAF Harvard Dataverse (<https://doi.org/10.7910/DVN/9HoKEE>). Five different vegetation classes were classified and sampled within the ranch: *Acacia drepanolobium* bushland (ADB) ($n = 16$ plots), arid zone mixed *Acacia* bushland (AZMAB) ($n = 13$ plots), open *Acacia brevispica* thicket (ABT) ($n = 104$ plots), grasslands (GR) ($n = 7$ plots) and Mpala

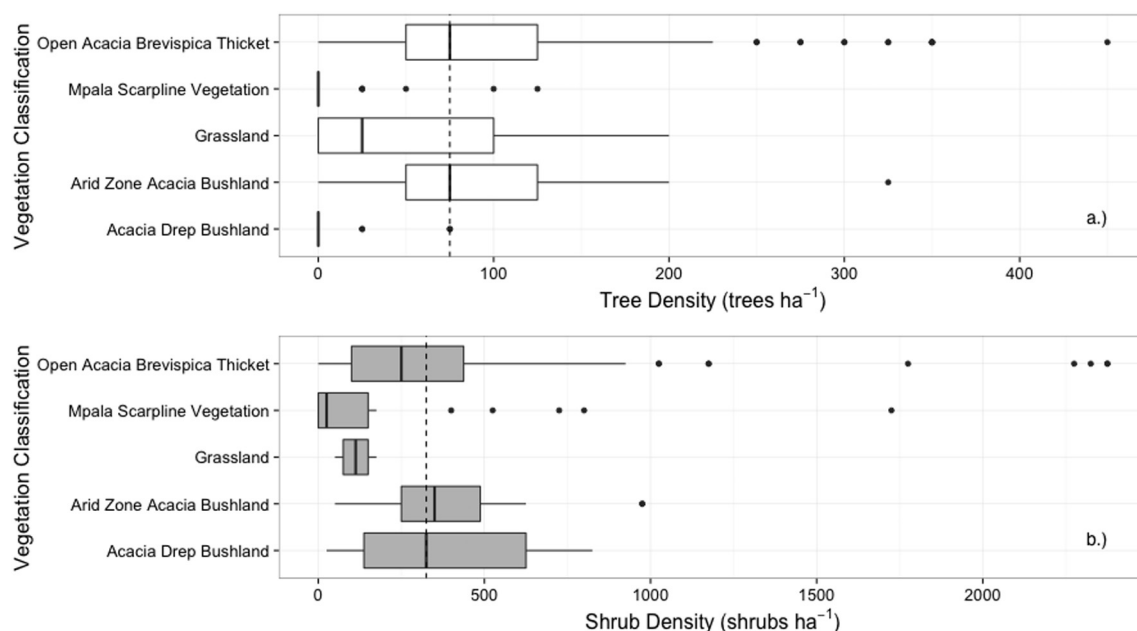


Fig. 2. Boxplot of tree densities (a) and shrub densities (b) in the five different vegetation classes within the Mpala Ranch. The vertical lines show overall average tree and shrub densities, respectively.

scarpline vegetation (MSV) ($n = 17$ plots). We calculated average tree and shrub densities for each of the five Mpala vegetation classes in order to describe the structure of the vegetation (Fig. 2). Overall, the average tree density for the surveyed plots was 75 trees ha^{-1} with open *Acacia brevispica* thicket (ABT) and arid zone *Acacia* Bushland (AZAB) having the highest tree densities compared to the other vegetation classes. This is most likely explained by this dominance of *Acacia brevispica* in ABT and *Acacia etbaica* and *Acacia mellifera* in AZAB. MSV and ADB vegetation classes had low tree densities (20 and 6 tree ha^{-1} , respectively). Average shrub density for the site was $325 \text{ shrubs ha}^{-1}$ with AZAB and ADB having the highest overall shrub densities. The relatively low tree densities and high shrub densities in areas with *Acacia drepanolobium* are consistent with a previous vegetation assessments in the whistling thorn (*Acacia drepanolobium*) vegetation class on black cotton soil, which found that 92–95% of the *Acacia drepanolobium* were < 4 m tall (Young et al., 1997). This means that a large proportion of these species are classified as shrubs in the LDSF as they are < 3 m tall. These data highlight structural variation across the vegetation classes.

3.2. Soil functional properties

Infrared spectroscopy is a well-established methodology for predicting soil properties such as SOC, pH, base cations, total nitrogen (TN) and texture (Brown et al., 2006; Madari et al., 2006; Reeves III et al., 2006; Shepherd and Walsh, 2002; Terhoeven-urselmans et al., 2010; Vågen et al., 2006), and as expected prediction model accuracy was very good for the soil samples collected at the Mpala ranch (Fig. 3). When assessing the relationship between measured and predicted values for each soil property, using the 32 reference topsoil and subsoil samples from the Mpala site, r^2 values were 0.98 for SOC, 0.98 for TN, 0.96 for pH, 0.98 for exchangeable bases, and 0.96 for clay. These results are better than those reported by Terhoeven-urselmans et al., 2010 for a globally distributed library of soil laboratory spectra, mostly due to the much larger sample size available for model development in our study and consistent laboratory methods for all samples used. The results presented in the following sections are derived from MIR-predicted soil property values.

Soil fertility has important implications for overall land

productivity. Table 1 shows a summary of key soil fertility indicators such as SOC, TN, pH, exchangeable bases (Ex Bases) and clay content for the Mpala site. The soils in the study area had high variability, with topsoil pH ranging from 5.5 to 8.3 and exchangeable bases from 5.75 to $65.99 \text{ cmol}_c \text{ kg}^{-1}$ (Table 1). The high exchangeable bases were related to sodic soils, which also have high pH, as shown in Fig. 4. Such soils include the locally classified black cotton soil type (Fig. 4). Fig. 4 also shows that the locally classified red soil had low pH values and that the locally classified transition soil spanned the range of both pH and exchangeable bases. In total, 120 plots were sampled in the red soil type, 15 plots in the black cotton soil type and 22 plots in the transition soil type. Average topsoil OC was 11.20 ± 4.55 ($n = 157$) and average subsoil OC was 8.76 ± 2.78 ($n = 132$) (Table 1). The relatively low SOC contents of the soils in this study are common in semi-arid systems, as reported in other studies including by (Glaser et al., 2001) for degraded and non-degraded savanna woodlands in semi-arid northern Tanzania (13.1 and 21.3 g C kg^{-1} , respectively). Results from other semi-arid savanna LDSF sites in Ethiopia, such as Mega and Merar, had average SOC values of 20.0 and 25.2 g kg^{-1} , respectively. The Merar site was dominated by Vertisols, which explains the higher SOC values (Tor-G Vågen et al., 2013). Studies on the carbon sequestration potential of dryland systems indicate that low net primary productivity in drylands is often due to low SOC and TN (Lal, 2004). While the soils of the Mpala study area do not have critically low SOC (defined as $< 5 \text{ g kg}^{-1}$ by the UNCCD), the effects of erosion on SOC was quite strong within the study area, with an average topsoil OC of 10.4 g kg^{-1} in severely eroded plots ($n = 121$) versus 13.5 g kg^{-1} in non-eroded plots ($n = 36$). The effect of erosion was strongest in grassland and open *Acacia brevispica* thicket (ABT) plots (Fig. 5). These results highlight the importance for reducing soil erosion, across all the vegetation classes as a mechanism for stabilizing and increasing SOC content. Total N values were low across the site, with about 99% of the samples falling below a critical threshold of $0.2 \text{ g kg}^{-1} \text{ N}$ in topsoil, indicating relatively low potential productivity. These N values also correspond to previous studies on N content in Mpala soils, which have been reported to be about 0.1% in topsoil (0–15 cm) collected from semi-arid bushlands surrounding bomas (Augustine, 2003). Several studies also assessed seasonal N dynamics in grassland systems in order to inform optimized grazing intensities for livestock, using soil N mineralization, litter

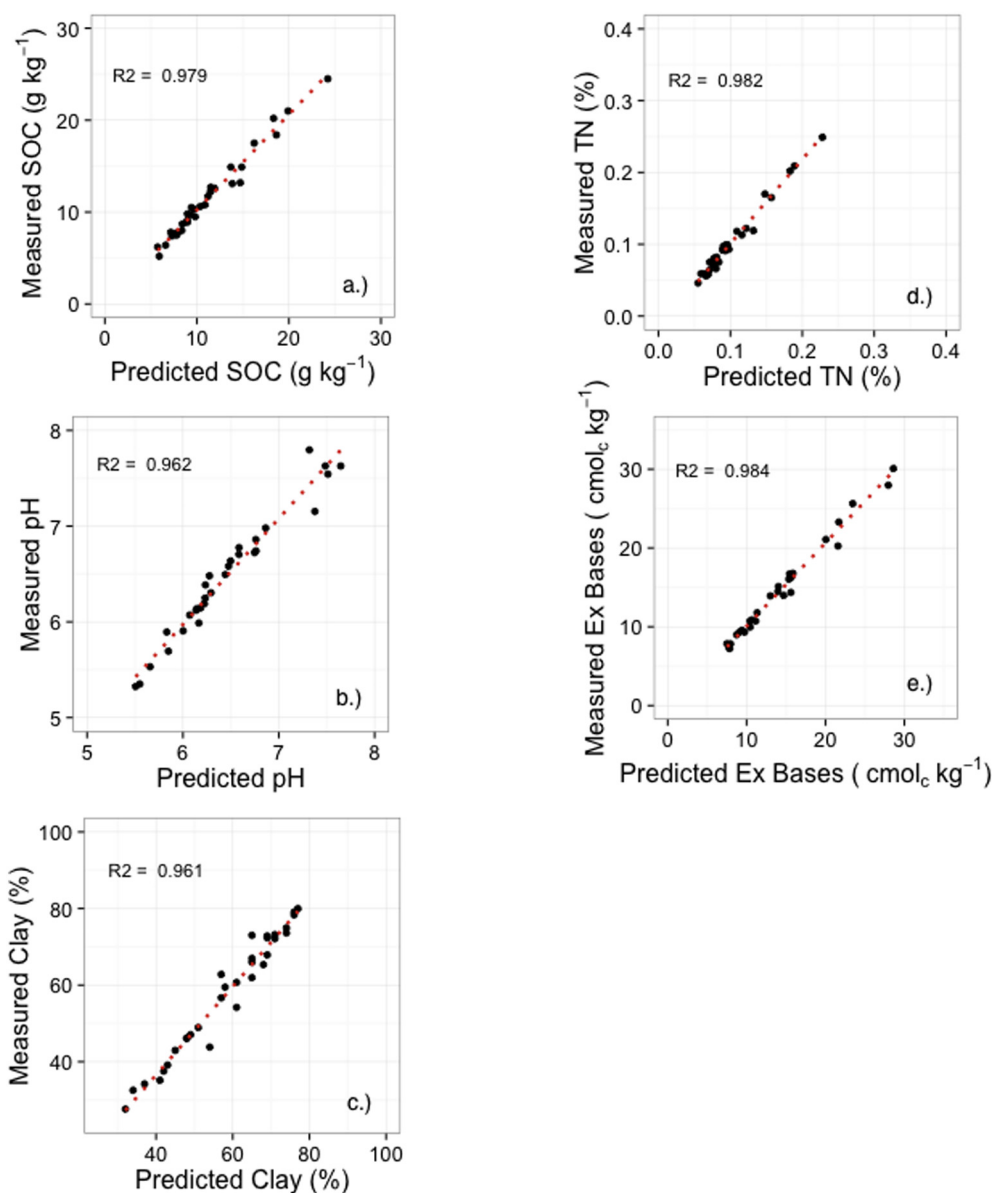


Fig. 3. Predicted versus measured soil properties based on MIR absorbance.

Table 1

Summary of soil health variables for the 157 plots sampled in the Mpala LDSF, by topsoil and subsoil, respectively. Ranges are shown in brackets after the means. These are the predicted values from the MIR spectra.

	SOC (g kg ⁻¹)	Total nitrogen (%)	pH	Ex bases (cmol _c kg ⁻¹)	Clay (%)
Topsoil (0–20 cm) (n = 157)	11.20 (5.07–28.92)	0.100 (0.039–0.189)	6.44 (5.51–8.26)	15.06 (5.75–65.99)	56 (27–76)
Subsoil (20–50 cm) (n = 132)	8.76 (3.59–22.66)	0.084 (0.048–0.228)	6.61 (5.49–8.47)	17.70 (5.80–56.84)	59 (25–77)

decomposition quality and rates and C:N ratios (Augustine and McNaughton, 2004; Frank and Groffman, 1994; Shariff et al., 1994).

3.3. Effects of vegetation types on SOC

We found a weak effect of vegetation class on SOC overall ($F = 2.037$, $df = 4$, 91.377 , $P = 0.096$). However, the highest SOC values were under ADB and MSV vegetation types, while open ABT and AZAB had lower SOC (Fig. 5). Young et al. (1998) identified five species

of perennial bunchgrass in the ADB vegetation class on Mpala. The higher SOC values in *Acacia Drepanolobium* are likely due to a combination of inherent soil properties, such as high clay content, as well as dense herbaceous cover. Erosion prevalence had a strong effect on topsoil SOC, with decreasing SOC in more eroded areas. The effects of erosion were more pronounced in grassland areas (Fig. 5) where severely eroded plots had very low SOC. Increasing herbaceous cover densities had a positive effect on SOC ($F = 4.114$, $df = 4$, 37.59 , $P = 0.007$) (Fig. 6) and SOC was significantly higher in plots with

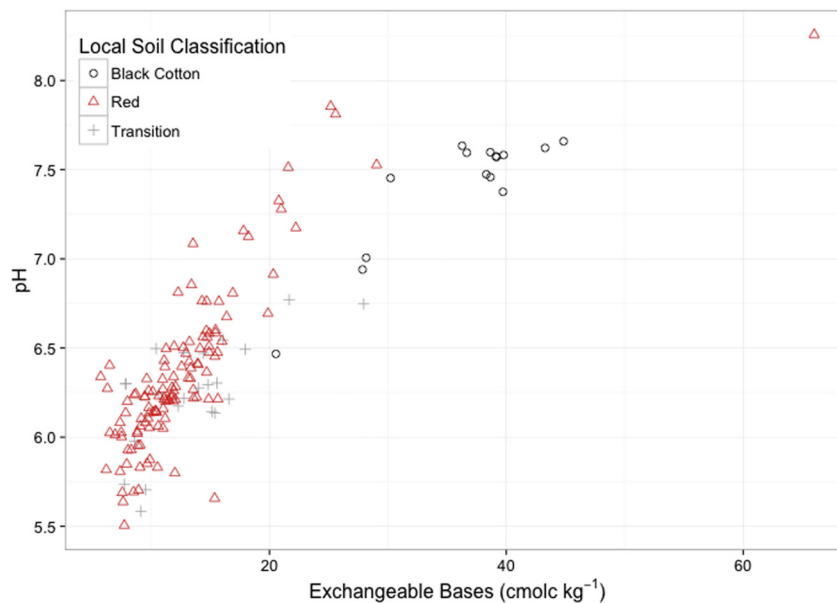


Fig. 4. Relationship between pH and exchangeable bases by local soil classification in the Mpala site.

woody cover > 40% ($F = 31.282$, $df = 1$, 116.09 , $P < 0.001$) indicating interaction effects between woody and herbaceous cover (Fig. 6). These findings have important implications for management of these rangelands, including specific interventions to rehabilitate woody and herbaceous cover.

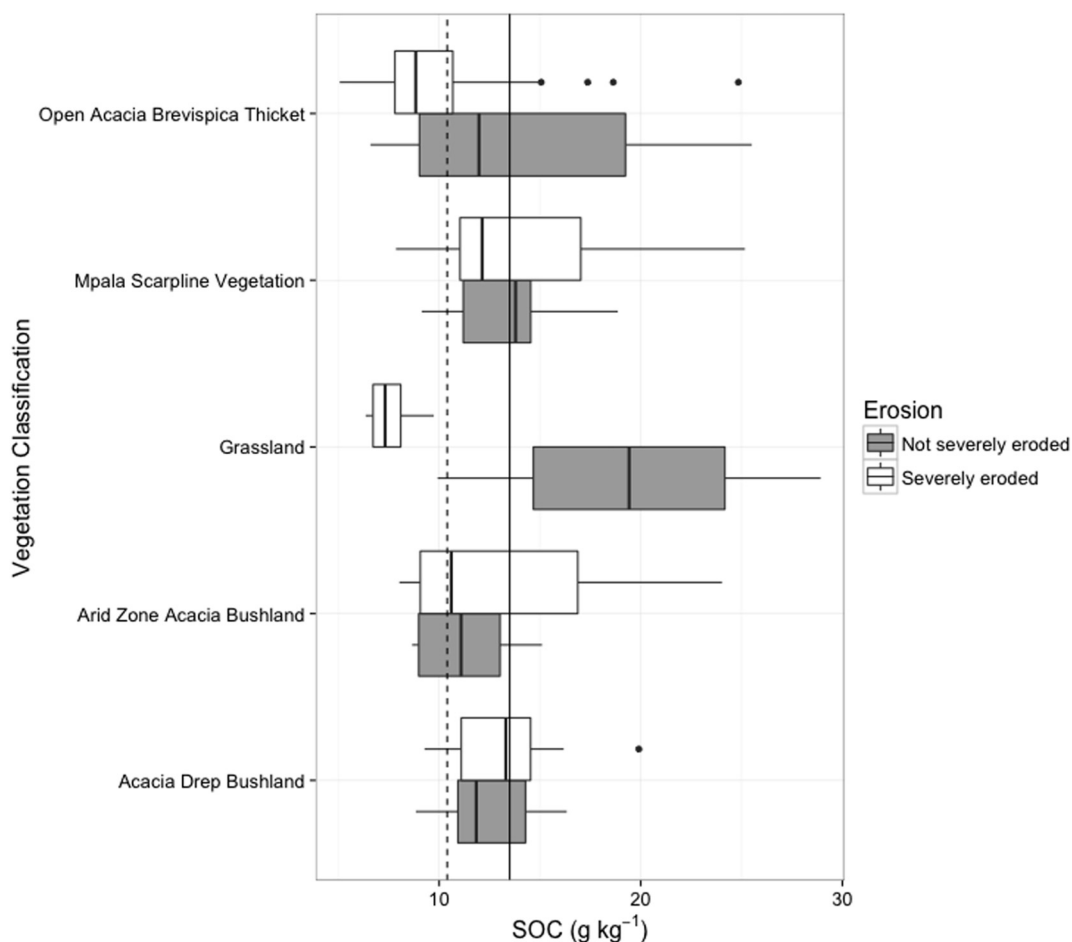


Fig. 5. Topsoil SOC values by vegetation class: Vertical lines show average SOC in severely eroded plots ($n = 126$, $SOC = 10.4 \text{ g kg}^{-1}$) and plots where no erosion was observed ($n = 31$, $SOC = 13.5 \text{ g kg}^{-1}$), respectively.

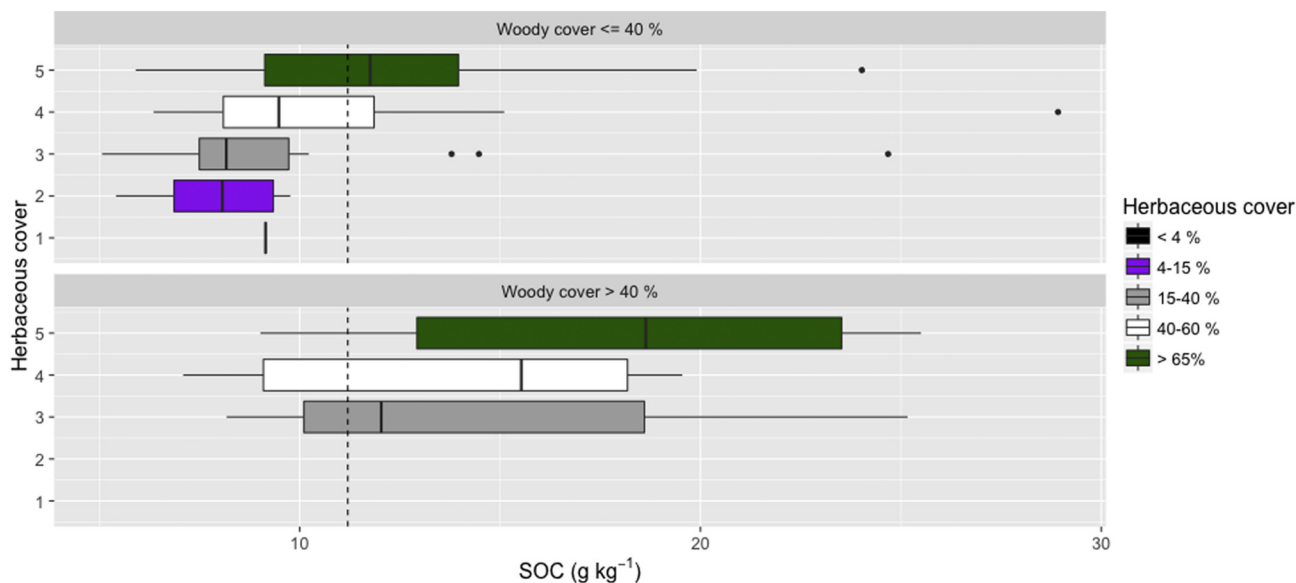


Fig. 6. Boxplots of topsoil OC values for different herbaceous cover ratings, split by woody cover higher than 40% (top) and lower than or equal to 40% (bottom). The vertical line shows average SOC for the site (11.2 g kg⁻¹).

3.4. Prediction and mapping of SOC based on Landsat 8

We tested the RF prediction model for SOC on a validation dataset ($n = 6936$ plots) with results showing a RMSEP of 9.12 g C kg⁻¹ and a r^2 of 0.84 (Fig. 7), or in other words good predictive performance overall. We therefore applied the SOC prediction model to a Landsat 8 scene from January 2015 for the Mpala Ranch. As can be seen in Fig. 8, the map of SOC for Mpala shows a decrease when going from south to

north. The higher SOC values in the southern part of the study area correspond to areas with the black cotton soil type, as well as areas with dense vegetation cover along the MSV, compared to the lower SOC values in the drier north, which was predominantly AZAB (Fig. 1). Fine-scale variations in SOC can be seen across the ranch, with spatial patterns that are associated with both woody and herbaceous cover densities and land degradation status, as discussed earlier.

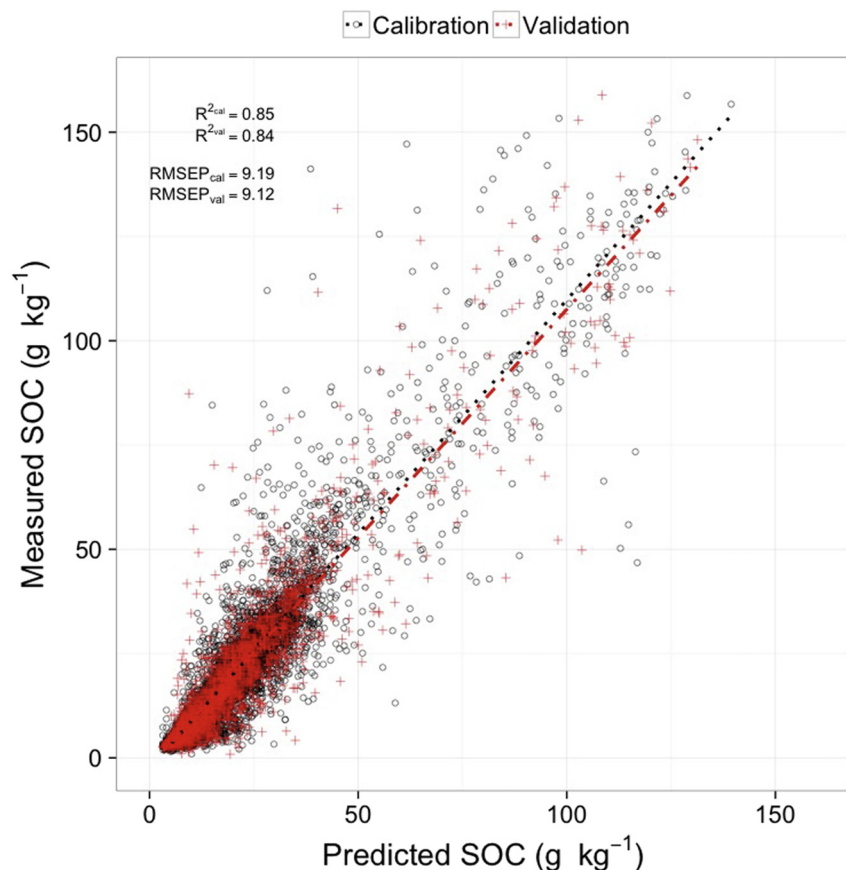


Fig. 7. Predicted vs measured SOC for calibration and validation model runs, respectively. The black dotted line shows the regression line for calibration model predictions, while the red dashed line shows the regression line for the validation model predictions. (For interpretation of the references to color in this figure legend, the reader is referred to the web version of this article.)

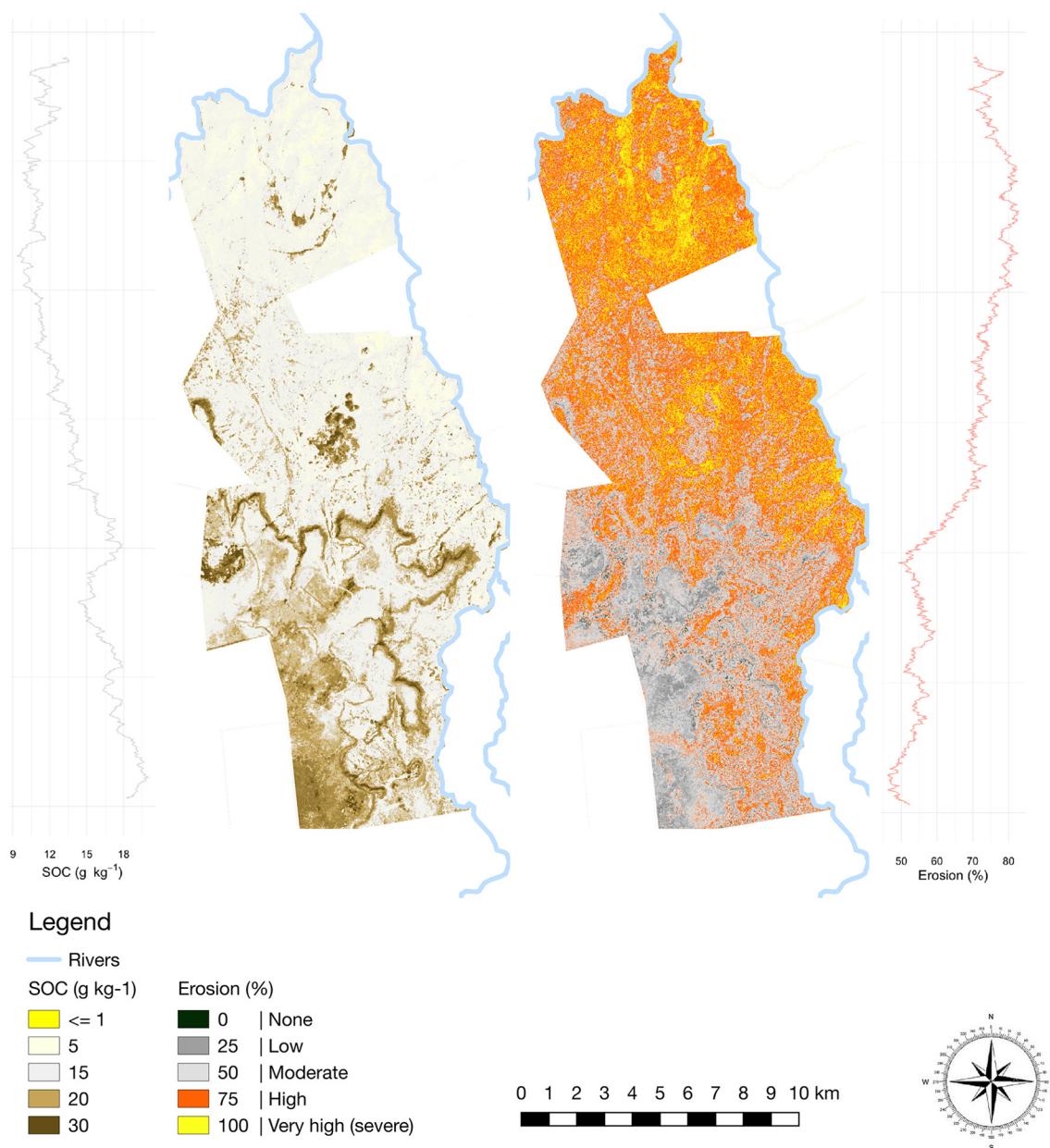


Fig. 8. Maps of SOC (left) and erosion prevalence (right) for Mpala, based on Landsat 8 imagery from January 2015. The graph to the left of the SOC map shows average SOC for each line (row) in the map going from the south to the north of the study area. Similarly, the graph to the right of the erosion map shows the average probability of erosion for each line (row) in the map of soil erosion predicted values for the study area, going from south to north across the conservancy.

3.5. Prediction and mapping of soil erosion based on Landsat 8

Prediction model performance for soil erosion was good (Fig. 9), with an overall accuracy of about 85% ($\text{AUC} = 0.87$ – Fig. 10). The ROC curve in Fig. 10, also shows good model precision and we therefore proceeded to predict erosion prevalence for Mpala based on the same satellite imagery used for predicting SOC. About 77% of the Mpala ranch is eroded, or has more than a 50% probability of erosion based on our predictions. If we consider only areas that have erosion prevalence higher than or equal to 75%, about 36% of the ranch is eroded. The map of erosion in Fig. 8 shows lower erosion in the southern part of the ranch, particularly on black cotton soils in the south-western part of the study area. The most important erosion hot-spots are found in the central and northern sections of Mpala, and along some of the riverbanks. As can be seen from the line graph to the right of the erosion map in Fig. 8, erosion prevalence increases quite dramatically north of the Mpala scarpline.

3.6. Mapping of land restoration potential

Land restoration potential was mapped at 30-m resolution, combining estimates of SOC and soil erosion prevalence. Areas with $> 20 \text{ g C kg}^{-1}$ and $< 50\%$ erosion prevalence were classified as areas that do not need immediate restoration, while areas with SOC between 10 and 20 g C kg^{-1} and erosion between 50 and 75% were considered areas of high restoration potential, needing moderate efforts to restore. Finally, areas with $< 10 \text{ g C kg}^{-1}$ and $> 75\%$ erosion were classified as areas in critical need of restoration, and with a high level of effort required. As highlighted earlier, these indicators of land degradation (soil erosion prevalence) and soil health (SOC) were influenced by aboveground vegetation, including woody and herbaceous cover, as well as climatic factors. Given the important interaction effects of woody and herbaceous cover on soil erosion reported earlier, restoration efforts need to consider herbaceous and woody cover, as well as vegetation type and diversity. Low overall SOC values and high

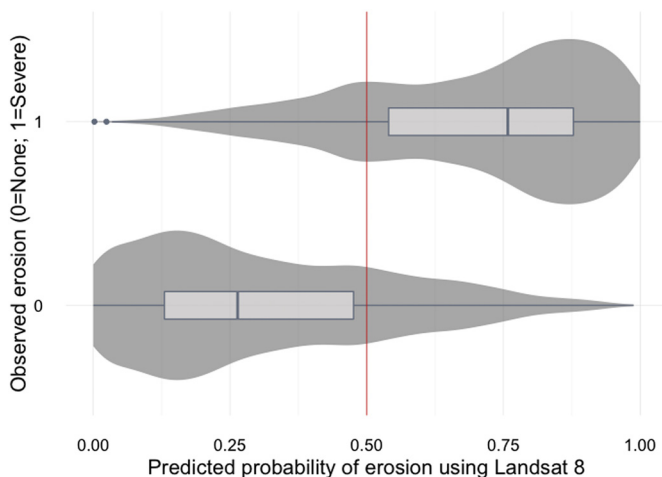


Fig. 9. The distribution of predicted probabilities (prevalence) of soil erosion for plots with observed erosion and plots where no erosion was observed in the field.

erosion prevalence were key biophysical constraints across the study area. The northern and northeastern regions of Mpala were mapped as areas requiring a high level of effort to restore. These areas have a drier climate and low fractional vegetation cover and may in some cases become irreversibly degraded unless interventions are implemented urgently. Areas classified as having no immediate need for restoration

correspond with areas that have higher fractional vegetation cover such as the Mpala Scarpline Vegetation class. As shown in Fig. 11, a large proportion of the Mpala Ranch can be considered degraded based on this analysis, but with moderate effort required for restoration. Interventions in these areas are critically needed to avoid further degradation and to restore ecosystem functions.

4. Conclusions

Semi-arid drylands are prone to land degradation. Increasing population and a degraded natural resource base continues to increase the pressure on these ecosystems. In response, several international, national and local efforts have dedicated resources to restoration of drylands. This study aimed to fill some of the gaps in spatially explicit information on land degradation in the semi-arid lands of Kenya in order to assess land degradation status and restoration potential, and inform restoration intervention efforts by focusing on a case study from the Mpala Ranch in Laikipia county. This study illustrated the utility of combining systematic field data collection with remote sensing to develop maps of restoration potential in the semi-arid lands of Kenya.

The results of our study showed that spatial variation in SOC and soil erosion prevalence was high across the Mpala. The effects of soil erosion on SOC were strong, decreasing SOC across all five vegetation classes in the study area, with the strongest effects in grasslands and open ABT plots. There were also strong effects of woody and herbaceous cover on topsoil OC, with higher SOC in plots with 40% or more woody cover and 15% or more herbaceous cover. There was also a

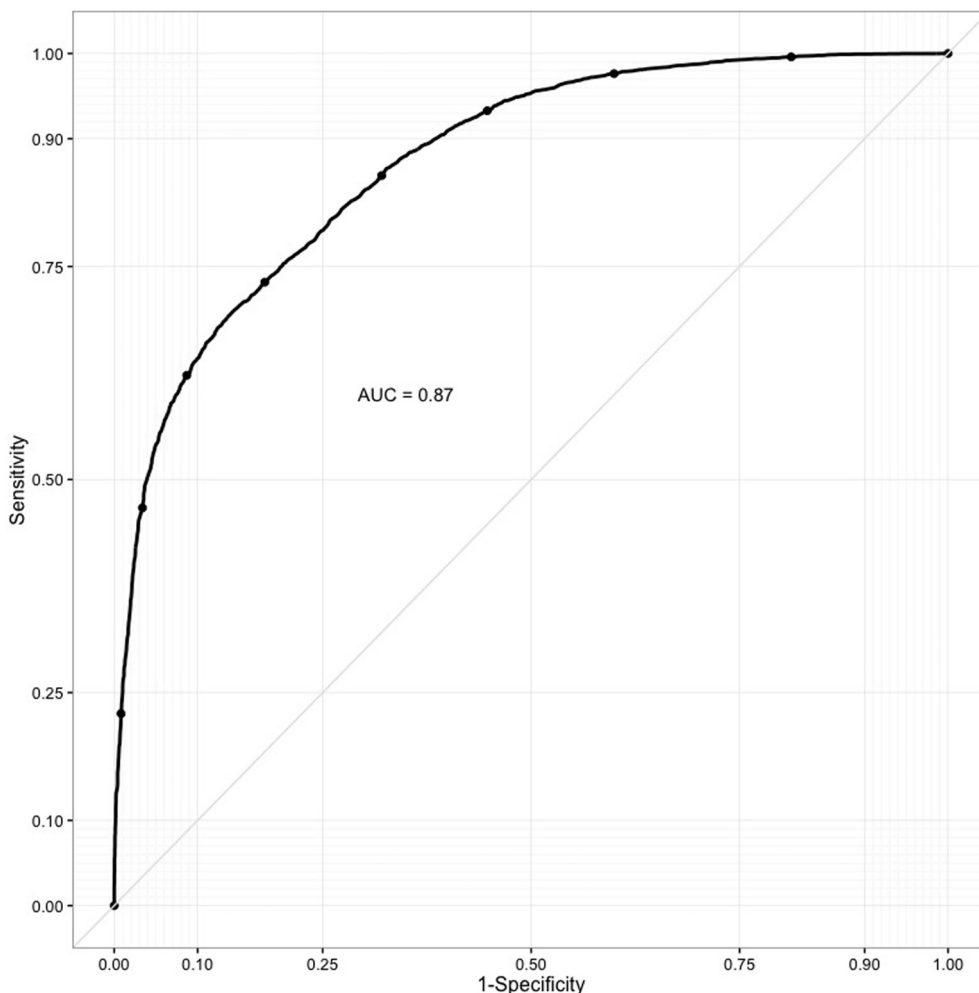


Fig. 10. Receiver operator characteristic (ROC) curve for the prediction of erosion.

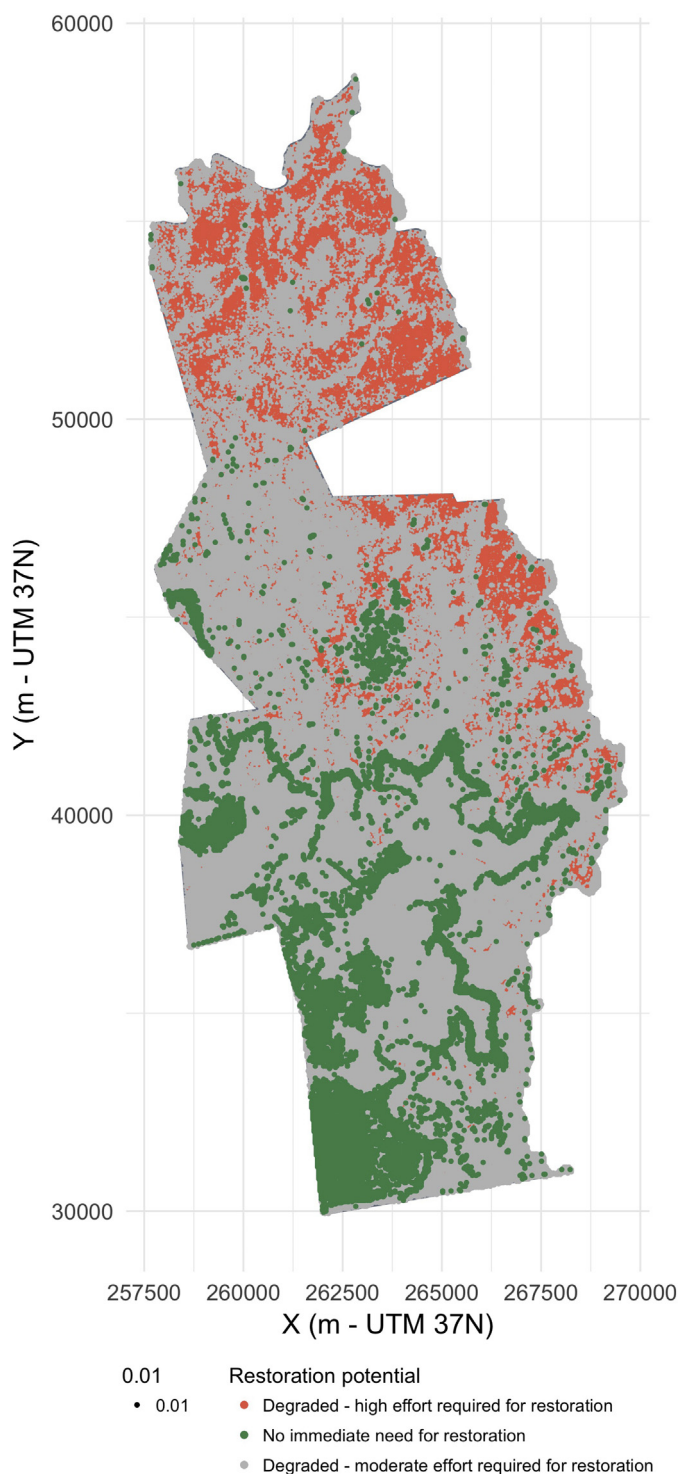


Fig. 11. Map of restoration potential for Mpala Ranch.

strong climatic gradient with decreasing rainfall from south to north of the Mpala Ranch, which corresponded to increasing erosion and decreasing SOC, respectively. These findings have important implications for the types of restoration activities that can potentially be carried out in semi-arid drylands of Kenya to restore ecosystem function, such as the need for specific efforts to increase both woody and herbaceous cover in order to increase SOC and reduce soil erosion. Further, appropriate grass species for each vegetation class need to be identified, ideally based on the degradation status of the area being restored. Previous studies have shown that the competition between grasses and

trees in *Acacia drepanolobium* areas on Mpala Ranch can limit tree growth, but with a lower degree of competition in areas with lower soil fertility (Riginos, 2009).

We developed three classes of restoration potential based on SOC and erosion prevalence. For example, areas with low degradation status and SOC concentrations higher than 20 g kg^{-1} were determined to not require immediate restoration. However, prevention of land degradation in these areas is needed. This class was mostly located in the southern part of the Mpala Ranch, particularly in areas with *Acacia Drepanolobium* on black cotton soil. Areas that had a high potential for restoration were defined as having moderate soil erosion and SOC values higher than 10 g kg^{-1} and $< 20 \text{ g kg}^{-1}$. These areas require moderate effort to restore as they will not have crossed critical thresholds of severe degradation. Finally, areas with high erosion prevalence ($> 75\%$) and low SOC ($< 10 \text{ g kg}^{-1}$) were classified as areas in critical need of restoration, but where a high level of effort will be required to restore SOC and other ecosystem functions. The map of restoration potential can be used to identify hotspots and to target restoration activities that maximize the multiple benefits and ecosystem functions of the landscape, taking into consideration required efforts, including for cattle ranching activities and wildlife conservation.

Acknowledgements

The authors would like to acknowledge the field team who implemented the LDSF field methodology in collaboration with the authors, including Grace Charles, Laura Budd, Francis Lomojo, Jackson Ekadeli and Wilson Longor. A special thanks to Corrina Riginos who also supported these efforts. Financial support was provided by a USAID grant to Improve Natural Resource Management and Biodiversity Conservation in Laikipia, Kenya (Cooperative Agreement No. AID 623-A-09-00002). Partial funding for the writing and analysis for the paper was provided by the International Fund for Agricultural Development (IFAD) Grant numbers 2000000520 and 2000000976 and the Drylands Systems and Forest Trees and Agroforestry CGIAR Research Programs.

References

- Ahn, P., Geiger, L., 1987. Kenya Soil Survey—Soils of Laikipia District. Kabete, Kenya.
- Aronson, J., Alexander, S., 2013. Ecosystem restoration is now a global priority: time to roll up our sleeves. *Restor. Ecol.* 21, 293–296. <http://dx.doi.org/10.1111/rec.12011>.
- Augustine, D.J., 2003. Long-term, livestock-mediated redistribution of nitrogen and phosphorus in an East African savanna. *J. Appl. Ecol.* 40, 137–149.
- Augustine, D.J., McNaughton, S.J., 2004. Temporal asynchrony in soil nutrient dynamics and plant production in a semiarid ecosystem. *Ecosystems* 7, 829–840. <http://dx.doi.org/10.1007/s10021-004-0253-1>.
- Batjes, N.H., 2004. Soil carbon stocks and projected changes according to land use and management: a case study for Kenya. *Soil Use Manag.* 20, 350–356. <http://dx.doi.org/10.1079/Sum2004269>.
- Berthold, M.R., Cebon, N., Dill, F., Gabriel, T.R., Kötter, T., Meinel, T., Ohl, P., Sieb, C., Thiel, K., Wiswedel, B., 2007. KNIME: The {K}onstanz {I}nformation {M}iner. In: Preisach, C., Burkhardt, H., Schmidt-Thieme, L., Decker, R. (Eds.), *Data Analysis, Machine Learning and Applications: Proceedings of the 31st Annual Conference of the Gesellschaft Für Klassifikation e.V.*, Albert-Ludwigs-Universität Freiburgand. Springer, Berlin, pp. 319–326.
- Braun-Blanquet, J., 1932. *Plant Sociology: The Study of Plant Communities*. McGraw-Hill, New York.
- Breiman, L., 2001. Random forests. *Mach. Learn.* 45, 35. <http://dx.doi.org/10.1023/A:1010933404324>.
- Brown, D.J., 2007. Using a global VNIR soil-spectral library for local soil characterization and landscape modeling in a 2nd-order Uganda watershed. *Geoderma* 140, 444–453. <http://dx.doi.org/10.1016/j.geoderma.2007.04.021>.
- Brown, D.J., Shepherd, K.D., Walsh, M.G., Mays, M.D., Reinsch, T.G., 2006. Global soil characterization with VNIR diffuse reflectance spectroscopy. *Geoderma* 132, 273–290. <http://dx.doi.org/10.1016/j.geoderma.2005.04.025>.
- Cowie, A.L., Orr, B.J., Castillo Sanchez, V.M., Chasek, P., Crossman, N.D., Erlewein, A., Louwagie, G., Maron, M., Metternicht, G.I., Minelli, S., Tengberg, A.E., Walter, S., Welton, S., 2018. Land in balance: The scientific conceptual framework for Land Degradation Neutrality. *Environ. Sci. Pol.* 79, 25–35. <http://dx.doi.org/10.1016/j.envsci.2017.10.011>.
- Crouzeilles, R., Curran, M., Ferreira, M.S., Lindenmayer, D.B., Grelle, C.E.V., Rey Benayas, J.M., 2016. A global meta-analysis on the ecological drivers of forest restoration success. *Nat. Commun.* 7, 1–8. <http://dx.doi.org/10.1038/ncomms11666>.
- Darkoh, M.B.K., 1998. *The nature, causes and consequences of desertification in the*

- drylands of Africa. *Land Degrad. Dev.* 9, 1–20.
- Davies, J., Poulson, L., Schulte-Herbruggen, B., Mackinnon, K., Crawhall, N., Henwood, W.D., Dudley, N., Smith, J., Gudka, M., 2012. *Conserving Dryland Biodiversity*.
- De Leeuw, J., Njenga, M., Wagner, B., Iiyama, M., 2014. *Treesilience: AN Assessment of the Resilience Provided by Trees in the Drylands of Eastern Africa*. (Nairobi).
- Di Gregorio, A., Jansen, L.J.M., 1998. *Land Cover Classification System (LCCS): Classification Concepts and User Manual*. (Rome).
- Dobson, A.P., Bradshaw, A.D., Baker, J.M., 1997. Hopes for the Future: Restoration Ecology and Conservation Biology. *Science* (277), 515–522. <http://dx.doi.org/10.1126/science.277.5325.515>. (80-).
- Dregne, H.E., 2002. Land degradation in the drylands. *Arid Land Res. Manag.* <http://dx.doi.org/10.1080/153249802317304422>.
- FAO, 2015. *Global Guidelines for the Restoration of Degraded Forests and Landscapes in Drylands: Building Resilience and Benefiting Livelihoods* (No. Forestry Paper No. 175). Rome.
- Frank, D.A., Groffman, P.M., 1994. Ungulate vs landscape control of soil C and N processes in grasslands of Yellowstone National Park. *Ecology* 79, 2229–2241.
- Georgiadis, N.J., Ihwagi, F., Olwero, J.N., Romañach, S.S., 2007. Savanna herbivore dynamics in a livestock-dominated landscape. II: ecological, conservation, and management implications of predator restoration. *Biol. Conserv.* 137, 473–483. <http://dx.doi.org/10.1016/j.biocon.2007.03.006>.
- Glaser, B., Lehmann, J., Führböter, M., Solomon, D., Zech, W., 2001. Carbon and nitrogen mineralization in cultivated and natural savanna soils of Northern Tanzania. *Biol. Fertil. Soils* 33, 301–309. <http://dx.doi.org/10.1007/s003740000324>.
- Herrick, J.E., Urama, K.C., Karl, J.W., Boos, J., Johnson, M.-V.V., Shepherd, K.D., Hempel, J., Bestelmeyer, B.T., Davies, J., Guerra, J.L., Kosnik, C., Kimiti, D.W., Ekai, a.L., Muller, K., Norfleet, L., Ozor, N., Reinsch, T., Sarukhan, J., West, L.T., 2013. The global Land-Potential Knowledge System (LandPKS): supporting evidence-based, site-specific land use and management through cloud computing, mobile applications, and crowdsourcing. *J. Soil Water Conserv.* 68, 5A–12A. <http://dx.doi.org/10.2489/jswc.68.1.5A>.
- Ito, 2002. ITTO guidelines for the restoration, management and rehabilitation of degraded and secondary ITTO guidelines for the restoration, management and rehabilitation of. Organization 84.
- IUCN, WRI, 2014. *A Guide to the Restoration Opportunities Assessment Methodology (ROAM): Assessing Forest Landscape Restoration Opportunities at the National or Sub-national Level*. (Road-test Ed. 125pp).
- Karl, J.W., Herrick, J.E., 2010. Monitoring and assessment based on ecological sites. *Soc. Range Manag.* 32, 60–64. <http://dx.doi.org/10.2111/RANGELANDS-D-10-00082.1>.
- Kinnaird, M.F., O'Brien, T.G., 2012. Effects of private-land use, livestock management, and human tolerance on diversity, distribution, and abundance of large African mammals. *Conserv. Biol.* 26, 1026–1039. <http://dx.doi.org/10.1111/j.1523-1739.2012.01942.x>.
- Laikipia Wildlife Forum, 2012. *A Wildlife Conservation Strategy for Laikipia County (2012–2030)*. (Nanyuki).
- Lal, R., 2004. Carbon sequestration in dryland ecosystems. *Environ. Manag.* 33, 528–544. <http://dx.doi.org/10.1007/s00267-003-9110-9>.
- Lapstun, S., 2015. *Forest and landscape restoration*. *Unasylva* 66.
- Madari, B.E., Reeves, J.B., Machado, P.L., Guimarães, C.M., Torres, E., McCarty, G.W., 2006. Mid- and near-infrared spectroscopic assessment of soil compositional parameters and structural indices in two Ferralsols. *Geoderma* 136, 245–259. <http://dx.doi.org/10.1016/j.geoderma.2006.03.026>.
- Mehlich, A., 1984. Mehlich 3 soil test extractant: a modification of the Mehlich 2 extractant. *Commun. Soil Sci. Plant Anal.* 15, 1409–1416.
- Millennium Ecosystem Assessment, 2005. *Ecosystems and Human Well-Being: Desertification Synthesis*. (Washington D.C.).
- Mortimore, M., 2009. *Dryland Opportunities: A New Paradigm for People, Ecosystems and Development*. (Gland, London, Nairobi).
- Neely, C.L., de Leeuw, J., 2008. Home on the Range the Contribution of Rangeland Management to Climate Change Mitigation. pp. 333–346.
- Neely, C., Bunning, S., Wilkes, A., 2009. *Review of Evidence on Drylands Pastoral Systems and Climate Change*. Land and Water Discussion Paper, Rome.
- Nyamwamu, R.O., 2016. Implications of human-wildlife conflict on food security among smallholder agro-pastoralists: a case of smallholder maize (*Zea mays*) farmers in Laikipia. *World. J. Agric. Res.* 4, 43–48. <http://dx.doi.org/10.12691/wjar-4-2-2>.
- R Core Team, 2015. *R: A Language and Environment for Statistical Computing*. R Foundation for Statistical Computing.
- Reeves III, J., Follett, R., McCarty, G., Kimble, J., 2006. Can near or mid-infrared diffuse reflectance spectroscopy be used to determine soil carbon pools? *Commun. Soil Sci. Plant Anal.* 37, 2307–2325. <http://dx.doi.org/10.1080/00103620600819461>.
- Riginos, C., 2009. Grass competition suppresses savanna tree growth across multiple demographic stages. *Ecology* 90, 335–340. <http://dx.doi.org/10.1890/08-0462.1>.
- Riginos, C., Herrick, J., 2010. *Monitoring Rangeland Health: A Guide for Pastoralists and Other Land Managers in Eastern Africa*. (Nairobi, Kenya).
- Riginos, C., Porensky, L.M., Veblen, K.E., Odadi, W.O., Sensenig, R.L., Kimuyu, D., Keesing, F., Wilkerson, M.L., Young, T.P., 2012. Lessons on the relationship between livestock husbandry and biodiversity from the Kenya Long-term Exclusion Experiment (KLEE). *Pastor. Res. Policy Pract.* 2, 1–22. <http://dx.doi.org/10.1186/2041-7136-2-10>.
- Schwilch, G., Bestelmeyer, B., Bunning, S., Critchley, W., Herrick, J., Kellner, K., Liniger, H.P., Nachtergaele, F., Ritsema, C.J., Schuster, B., Tabo, R., van Lynden, G., Winslow, M., 2011. Experiences in monitoring and assessment of sustainable land management. *Land Degrad. Dev.* 22, 214–225. <http://dx.doi.org/10.1002/ldr.1040>.
- Schwilch, G., Liniger, H.P., Hurmi, H., 2014. Sustainable land management (SLM) practices in drylands: how do they address desertification threats? *Environ. Manag.* 54, 983–1004. <http://dx.doi.org/10.1007/s00267-013-0071-3>.
- Shariff, A.R., Biondini, M.E., Grygiel, C.E., 1994. Grazing intensity effects on litter decomposition and soil nitrogen mineralization. *Soc. Range Manag.* 47, 444–449.
- Shepherd, K.D., Walsh, M.G., 2002. Development of reflectance spectral libraries for characterization of soil properties. *Soil Sci. Soc. Am. J.* 66, 988–998.
- Suding, K., Higgs, E., Palmer, M., Callicott, J.B., Anderson, C.B., Baker, M., Gutrich, J.J., Hondula, K.L., LaFevor, M.C., Larson, B.M.H., Randall, A., Ruhl, J.B., Schwartz, K.Z.S., 2015. Committing to ecological restoration. *Science* 348, 638–640. <http://dx.doi.org/10.1126/science.aaa4216>. (80-).
- Terhoeven-urselmans, T., Vagen, T., Spaargaren, O., Shepherd, K.D., 2010. Prediction of soil fertility properties from a globally distributed soil mid-infrared spectral library. *Soil Sci. Soc. Am. J.* 74. <http://dx.doi.org/10.2136/sssaj2009.0218>.
- Tiffen, M., Mortimore, M., 2002. *Questioning Desertification in Dryland Sub-Saharan Africa*. 26. pp. 218–233.
- UNCCD-GM, 2016. *Achieving Land Degradation Neutrality at the country level: Building blocks for LDN target setting*. In: *Global Mechanism (GM) of the United Nations Conventions to Combat Desertification (UNCCD)*, Bonn, Germany Available online: [https://www2.unccd.int/sites/default/files/documents/160915_ldn_rgb_small%20\(1\).pdf](https://www2.unccd.int/sites/default/files/documents/160915_ldn_rgb_small%20(1).pdf).
- Vågen, T.-G., Gumbrecht, T., 2012. *Sahel Atlas of Changing Landscapes: Tracing Trends an Variations in Vegetation Cover and Soil Condition, 1st ed*. UNEP, Nairobi, Kenya.
- Vågen, T.-G., Winowiecki, L.A., 2013. Mapping of soil organic carbon stocks for spatially explicit assessments of climate change mitigation potential. *Environ. Res. Lett.* 8, 15011. <http://dx.doi.org/10.1088/1748-9326/8/1/015011>.
- Vågen, T.-G., Shepherd, K.D., Walsh, M.G., 2006. Sensing landscape level change in soil fertility following deforestation and conversion in the highlands of Madagascar using Vis-NIR spectroscopy. *Geoderma* 133, 281–294. <http://dx.doi.org/10.1016/j.geoderma.2005.07.014>.
- Vågen, T.-G., Davey, F.A., Shepherd, K.D., Nair, P.K.R., Garrity, D., 2012. Land health surveillance: mapping soil carbon in Kenyan rangelands. In: *The Future of Global Land Use: Advances in Agroforestry*. Springer Science, pp. 455–462. <http://dx.doi.org/10.1007/978-94-007-4676-3>.
- Vågen, T.-G., Winowiecki, L.A., Abegaz, A., Hadgu, K.M., 2013a. Landsat-based approaches for mapping of land degradation prevalence and soil functional properties in Ethiopia. *Remote Sens. Environ.* 134, 266–275.
- Vågen, T.-G., Winowiecki, L.A., Tamene Desta, L., Tondoh, J.E., 2013b. *The Land Degradation Surveillance Framework (LDSF) - Field Guide v3*, World Agroforestry Centre (ICRAF). World Agroforestry Centre, Nairobi, Kenya.
- Vågen, T.-G., Winowiecki, L.A., Tondoh, J.E., Desta, L.T., Gumbrecht, T., 2016. Mapping of soil properties and land degradation risk in Africa using MODIS reflectance. *Geoderma* 263, 216–225.
- Wand, M., 2015. *KernSmooth: Functions for Kernel Smoothing Supporting Wand & Jones* (1995).
- Williams-linera, G., Alvarez-Aquino, C., Suarez, A., Smith-Ramirez, C., Echeverria, C., Cruz-Cruz, E., Bolados, G., Armesto, J.J., Heinemann, K., Malizia, L., Becerra, P., Del Castillo, R.F., Urrutia, R., 2011. Experimental analysis of dryland forest restoration techniques. In: *Principles and Practice of Forest Landscape Restoration: Case Studies from the Drylands of Latin America*, pp. 131–182.
- Winowiecki, L., Vågen, T.-G., Huisling, J., 2016. Effects of land cover on ecosystem services in Tanzania: a spatial assessment of soil organic carbon. *Geoderma* 263, 274–283. <http://dx.doi.org/10.1016/j.geoderma.2015.03.010>.
- Young, T.P., Stubblefield, C.H., Isbell, L.A., 1997. Ants on swollen-thorn acacias: species coexistence in a simple system. *Oecologia* 109, 98–107.
- Young, T.P., Okello, B.D., Kinyua, D., Palmer, T.M., 1998. KLEE: a long-term multi-species herbivore exclusion experiment in Laikipia, Kenya. *Afr. J. Range Forage Sci.* 14, 94–102.
- Young, T.P., Petersen, D.A., Clary, J.J., 2005. The ecology of restoration: historical links, emerging issues and unexplored realms. *Ecol. Lett.* 8, 662–673. <http://dx.doi.org/10.1111/j.1461-0248.2005.00764.x>.